Lightweight Torque-Vectoring Transmission for the Electric Vehicle VISIO.M

Philipp Gwinner
Research Associate
Gear Research Center (FZG)
Dept. of Mechanical Engineering
Technische Universität München
Germany, Munich 85748
Email: gwinner@fzg.mw.tum.de

Michael Otto
Research Group Head
Gear Research Center (FZG)
Dept. of Mechanical Engineering
Technische Universität München
Germany, Munich 85748
Email: otto@fzg.mw.tum.de

Karsten Stahl
Full Professor
Gear Research Center (FZG)
Dept. of Mechanical Engineering
Technische Universität München
Germany, Munich 85748
Email: stahl@fzg.mw.tum.de

***Abstract*—To meet the challenging requirement of high efficiency for fully electric drive vehicles, lightweight design throughout the entire vehicle architecture becomes increasingly important. The high speeds of electric drives currently in use, and their low noise emission in comparison to conventional combustion engines require axle drives with acoustically low noise gear concepts. In this paper a novel axle drive concept for electric vehicles with a mechanical torque-vectoring functionality is presented. Conventional axle drives for automotive applications feature helical gears in order to ensure quiet operation of the power train, however, risking the consequence of additional axial forces in comparison to ordinary cylindrical gears. This causes higher loads on the shafts and housing and has to be considered during the design process to ensure an adequate load carrying capacity and low deformations of the components. In this paper an axle drive concept will be shown featuring no axial forces, so that the acting load on the gearbox system can be reduced explicitly. This approach permits a downsizing of the gearbox components and the application of lightweight materials. Thus, it is possible to utilize a housing made of a reinforced plastic material as well as plastic gears into the torque-vectoring system to significantly reduce the transmission weight. Generally, conventional axial force free spur gear designs, e. g. cylindrical gears, do not provide a beneficial acoustical excitation level in comparison to helical gear designs. Due to a specific gear layout, which is designed for the axle drive of the VISIO.M vehicle, the arithmetical noise excitation can be reduced and makes the use of innovative lightweight materials possible. The design of the presented lightweight transmission as well as the weight and the excitation level will be compared to former construction stages of the transmission.**

***Keywords*—torque-vectoring, electric vehicle, plastic gears, excitation level, active differential**

I. INTRODUCTION

At the Technische Universität München a network of 14 research institutes and associated industrial partners are developing a fully electric powered subcompact vehicle called VISIO.M (see Fig. 1). The related research project, which is the follow-up project of the MUTE project, started in March 2012 and is targeting to build up an optimized prototype vehicle in terms of costs, enhanced safety and high efficiency. The low priced and innovative vehicle is designed for 2 passengers and a suburban purpose. Related to the vehicle class $L7e$, the net weight (without battery and payload) of the vehicle is limited to $450\ kg$. The primary energy storage consists of a rechargeable lithium-ion-battery with a nominal capacity of $13.5\ kWh$, which guarantees a range of at least $100\ km$ considering an suburban-oriented driving cycle.

Fig. 1. Electric vehicle VISIO.M

Research project	**MUTE**	**Visio.M**	
Construction stage	CS01	CS02	CS03
Concept	2-stage axle gear torque-vectoring	2-stage axle gear torque-vectoring	2-stage axle gear torque-vectoring
Technology	state of the art	optimized	lightweight + optimized

Engineering Progress, Cost & Weight Reduction

Fig. 2. Transmission construction stages

The VISIO.M vehicle features a rear wheel drive due to the safety concept, the limited vehicle package and high requirements on driving dynamics. The power train consists of an asynchronous drive motor with a nominal driving power at the wheels of $15\ kW$ (restricted by the vehicle class $L7e$) and a maximum speed of $12,000\ rpm$ at a vehicle velocity of $120\ km/h$. The nominal power, which covers the load spectrum of characteristic suburban driving cycles, can be temporarily raised to a peak power of $30\ kW$, i. e. for acceleration driving conditions. The axle drive provides the speed and torque adaption of the drive motor to the wheels.

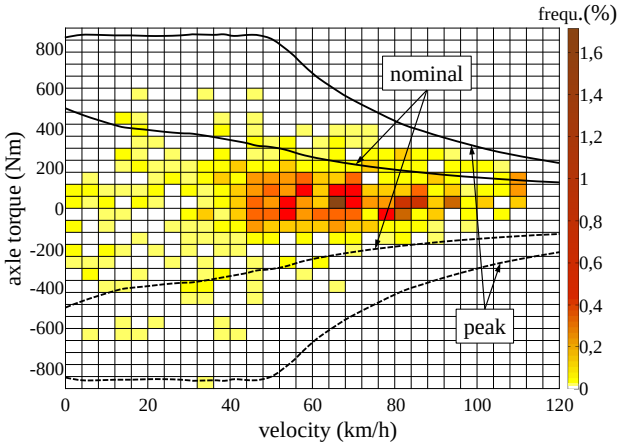

Fig. 3. Wheel axle load spectrum according to the Artemis Extra Urban driving cycle and characteristic of the drive motor in motor (continuous line) and recuperation operation (dashed line)

During the VISIO.M project two transmission construction stages have been developed and assembled (see Fig. 2), which feature the same interface architecture to the periphery, so that each of the two transmissions can be integrated into the VISIO.M power train. The first construction stage CS02 is mainly based upon the gearbox concept of the MUTE project [1], designed with conventional materials and gears and was optimized in terms of weight and costs. The design of the second construction stage CS03, which is discussed in detail in this paper, intensively focuses on reducing weight by changing the gear layout and applying alternative lightweight materials. In the following, the power train structure and the operating conditions of the vehicle are presented. The constructional details as well as the concept changes to former transmission construction stages will be discussed for the lightweight transmission CS03. The construction stages will be compared in terms of weight and costs. A further focus in this paper is put on the arithmetical gear excitation level of the axle drive, which has a significant influence on the total noise emission of fully electric powered vehicles. A major design criterion is to reduce the gearing excitation level, in particular for lower vehicle velocities, where wind and driving noise has a secondary influence on the noise perception of the the vehicle passengers. Therefore, the tooth flank profiles of the axle drive gears were modified systematically to reduce the excitation level of the gearings as well as to ensure a smooth load distribution on the tooth flanks. An arithmetical characteristic will be presented, which allows a qualitative correlation between the excitation level of a gearing and the vibration response of the system, i. e. the noise emission of the transmission.

II. VISIO.M Power Train

A. Operating Conditions

The VISIO.M vehicle features a rear wheel drive, as a result of the ambitious safety concept and high requirements referring to the driving dynamics, with a one-speed axle drive transmission and an additional torque-vectoring functionality

Fig. 4. VISIO.M power train with transmission CS02

(see Fig. 4). The torque-vectoring system, which is powered by an additional small synchronous electric machine, provides an individual torque distribution to each driven wheel at the rear axle and can be used for a variety of comfort and driving dynamics features. The power demand of the power train was designed for suburban vehicle use according to characteristic driving cycles. Fig. 3 exemplarily shows the load spectrum of the axle torque for the fully loaded vehicle according to the *Artemis Extra Urban* driving cycle. As one can see in Fig. 3, the power requirement of the vehicle is satisfied by the power capacity of the drive motor for drive (continuous line) and recuperation (dashed line) operation. The load frequency of the occurring operating conditions is highlighted with color and can be obtained by allocating the vehicle operating conditions of the driving cycle to discrete load levels (small boxes) of the load spectrum. The gears of the transmissions were designed according to this load spectrum, derived from the driving cycle respectively, in order to ensure a lightweight design in contrast to a fatigue endurable design. The mechanically applied torque-vectoring system allows to variably distribute the torque to each driven wheel by engaging actively into the differential with an interconnecting sun gear (see Fig. 5), whereas a conventional differential features a fixed torque distribution to the wheels of $50:50$. Therefore, an individual torque can be applied to each driven wheel according to the actual driving condition, so that several advantages [2] result in applying a torque-vectoring system, such as

- improvement of transverse driving dynamics (optimal torque at each driven wheel)
- traction enhancement (equivalent to a differential lock)
- increase of the recuperation potential (optimal brake torque at each wheel)
- driving comfort (e.g. cross wind compensation, lane groove assistant, power steering)

Further advantages of the application of torque-vectoring and control strategies are presented by [3], [4], [5], [6] and [7]. As the torque-vectoring unit is mainly loaded during cornering, the corresponding gearings of the superimposing unit were calculated assuming high loads (maximum available difference in torque at the wheels) with a reduced time slice of $50\ \%$ in contrast to the axle drive load spectrum. In summary, four different operating conditions of the power train are possible:

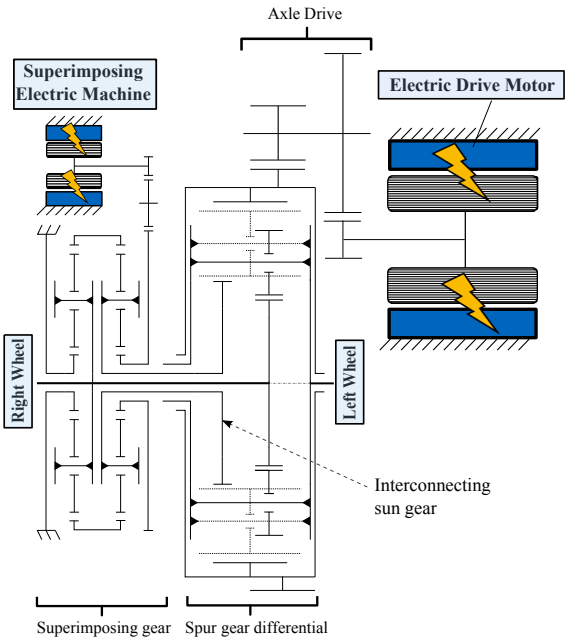

Fig. 5. VISIO.M power train – structure scheme

The drive motor is running in motor operation if the vehicle speed is kept constant or during acceleration with or without activated torque-vectoring (operating conditions 1 and 2). The 3^{rd} and 4^{th} operating condition is the recuperation mode, where the drive motor is running in generator operation with or without activated torque-vectoring. The torque-vectoring electric machine is running in generator and motor operation as well, depending on the direction of the wheels' speed. If torque is transferred to the faster running wheel, the torque-vectoring motor is running in motor operation and vice versa.

B. Layout and functioning

In principle, the transmission (CS02 & CS03) of the VISIO.M vehicle consists of three different assembly groups: the axle drive, the differential and the torque-vectoring unit (see Fig. 5). The axle drive of the CS02 is designed as a conventional two-stage spur gear train with helical gears and a total gear ratio of $i = 10.15$. The final drive contains a compact designed spur gear differential, which is mounted into the final drive featuring a planetary gear train of the *Ravigneaux* type. Further torque-vectoring transmissions are presented by [8], [9] and [10]. During straight ahead driving, the final drive as well as the differential gears rotate with the same absolute speed. During cornering the differential gears are rotating with a relative speed in comparison to the final drive wheel to allow the different speeds of the driven vehicle wheels. The differential gear ratio between the two wheel output shafts, which are the sun gear and the carrier shaft of the differential, is $i_{diff} = -1$ respectively. The axle torque is distributed conventionally by $50:50$ to the wheels, if the torque-vectoring unit is not activated. Due to the symmetrical layout of the superimposing unit, the superimposing electric machine stands still if the wheel speeds of the vehicle are identical, i. e. during straight ahead driving. Thus, the power losses of the torque-vectoring unit can be reduced. The differential torque

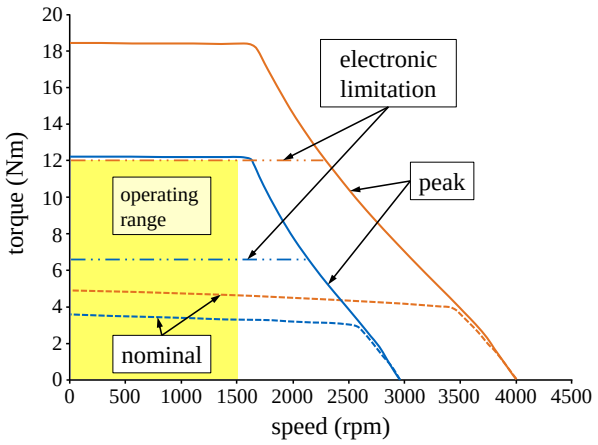

Fig. 6. Map of the superimposing electric machine for transmission CS02 (orange line) and CS03 (blue line)

ratio can be influenced or rather changed by actuating the superimposing electric machine of the torque-vectoring unit. Then, the interconnecting sun gear, which is engaging actively into the differential, is loaded and transfers torque from one driven wheel to another. To reduce the torque requirements of the superimposing electric machine, two identically constructed planetary gear trains are assembled into the torque-vectoring unit to provide a high superimposing gear ratio. Thus, it is possible to provide high differences in torque at the wheels using a small superimposing electric machine. In contrast to the MUTE transmission CS01, where one sun gear of the superimposing planetary gear train is directly driven by a hollow shaft electric machine, the superimposing unit of CS02 & CS03 features two pre-arranged cylindrical gear stages. These cylindrical gear stages are additionally implemented to the superimposing planetary gear train in order to further raise the superimposing gear ratio and to be able to mount a conventional and modular torque motor, which is available in different power classes and can easily be mounted to and dismounted from the transmission. The applied torque motor is available with a different face-to-face length and nominal power respectively.

The adjustable difference in torque at the wheels provided by the torque-vectoring unit is dependent on the gear ratio of the superimposing unit and the output torque of the superimposing electric machine. According to [2] the difference in torque at the driven wheels ΔT_{wheels} is defined as

$$\Delta T_{wheels} = i_{TV} \cdot T_{sem} \tag{1}$$

with the superimposing gear ratio i_{TV} and the torque of the superimposing electric machine T_{sem}. The speed of the superimposing electric machine is a function of the speed difference of the wheels and the superimposing gear ratio and reads:

$$n_{sem} = \frac{i_{TV}}{2} \cdot \Delta n_{wheels} \tag{2}$$

The superimposing planetary gears of the CS02 and CS03 have a gear ratio of 12 and the pre-arranged cylindrical gear stages a gear ratio of 4, so that the total superimposing gear ratio i_{TV} is 48. With an electronically limited peak torque of 12 Nm for the torque motor of the CS02 and 6.5 Nm of the CS03 (see Fig. 6), a maximum difference in torque at the wheels ΔT_{wheels} of 576 Nm and 312 Nm can be reached. As the superimposing electric machine is not actively cooled, the peak torque of the superimposing electric machine has to be limited electronically to ensure the availability of this torque for up to 10 seconds, e. g. if torque-vectoring is actuated in a long curve. Based on simulations, the maximum difference in speed at the wheels is determined to be 50 rpm for stable vehicle operating conditions, so that a maximum speed of 1200 rpm (according to Eq. 2) results at the superimposing electric machine. A further advantage of the additional cylindrical gear stages of the superimposing unit arises form the four times higher speeds of the superimposing machine in comparison to the torque-vectoring unit of the CS02, as the electric machine can be run in more beneficial operating speeds in terms of efficiency.

III. Design and Assembly of the Power Train

A. Axle Drive

The axle drive of each transmission designed during the MUTE and VISIO.M project features a two-stage spur gear train to lower the speed of the drive motor and lift the axle torque. The MUTE and first VISIO.M axle drive have helical gears to ensure low-noise running, whereas the CS03 axle drive provides axial force free gearings. If the aluminium housing of the CS01 & CS02 needs to be replaced by a lightweight housing, it is essential to reduce the acting load on the housing. In particular, bending torques acting perpendicular to the plane of the housing shell, caused by axial forces of the gearings, lead to undesirable high deformations and loads in the housing. Nevertheless, a gearing concept has to be designed that provides both a low-noise emission level and a compact and light design. Thus, a double helical gearing of the herringbone type was designed for both gear stages of the axle drive CS03 (Fig. 7), which ensures a very compact construction, no axial forces to be retained by the housing and a low acoustical excitation. The bearings of the axle drive do not have to retain axial forces as well, so that a very easy and light bearing concept can be applied. In order to ensure a free adjustability of the double helical gearings a floating bearing arrangement has to be attached, which has the further positive effect of an easy compensation of different thermal expansions of the steel shafts and plastic housing in operation. Only the final drive bearings are fixed to position the axle drive in the housing to ensure an accurate junction of the interconnecting shafts of the superimposing unit to the differential (Fig. 8).

The herringbone gears of the axle drive are realized with a two-part assembly, so that one gear half is cut directly into the shaft, whereas the other half is manufactured as a gear rim. Both parts are connected via a joining process, i. e. laser welding or a press fit. This process is conducted for each gear of the axle drives. A one-part solution for this transmission is not possible, as the gap between the two helical gear parts has to be kept small in terms of compactness. Then, a gear grinding is not possible anymore due to a limited minimal

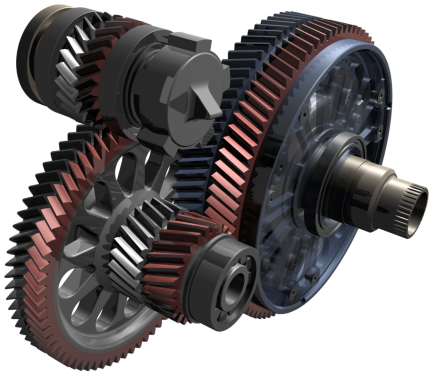

Fig. 7. Axle drive of transmission CS03 (drive motor not illustrated)

diameter of the grinding wheel. The two-part design ensures an easy manufacturing of the gears with conventional tools. Both gear halfs of a herringbone gear feature the same involute shape and profile modification.

A further challenge in the design of herringbone gears is the circumferential positioning of both parts to each other. Due to manufacturing and positioning tolerances the virtual extensions of both tooth flanks of a herringbone gear do not cut in the middle of both parts, so that the gear will execute an axial compensation motion to achieve a smooth load distribution on both parts (self-centering). Therefore, a floating bearing arrangement has to be applied to at least one wheel of a gearing to enable the axial movement of the shaft. The necessary gap between both parts of a gearing bone has to be large enough to ensure that, in the case of a compensation of one shaft, one part of the herringbone gear does not engage with the opposite part of the counter wheel.

B. Torque-Vectoring System

The power demand of the torque-vectoring unit was originally designed to reduce the total power losses at the wheels in recuperation mode during cornering ([1], [11]). The optimal torque distribution to each wheel, which is realized by the torque-vectoring system, stabilizes the vehicle during cornering in recuperation mode, as the traction potential at each wheel can be exploited to its maximum. Thus, the drive motor can retain higher torques and reaches higher recuperation levels in comparison to power trains without torque-vectoring functionality. Calculations with a numeric model of the MUTE vehicle showed that an nominal input power of the superimposing electric machine has to be about 1000 W to reach a difference in torque of 400 Nm at the wheels and the highest recuperation potential of the drive motor. For demonstration purposes the VISIO.M transmission CS02 features a super-

Fig. 8. Differential of transmission CS03

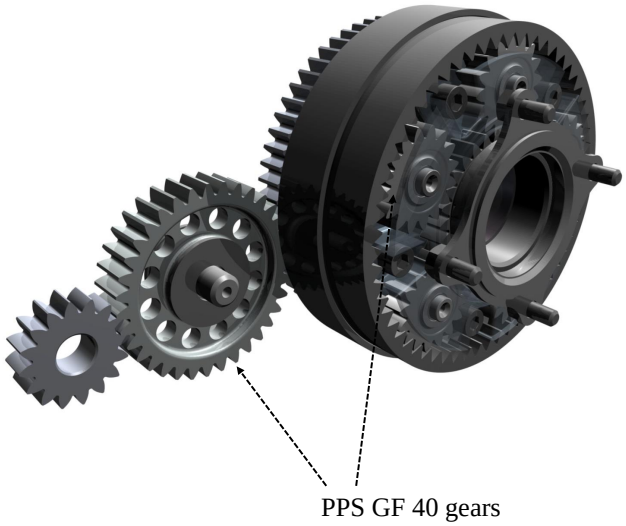

Fig. 9. Torque-vectoring unit of transmission CS03 with PPS GF 40 intermediate and planet gears (superimposing electric machine not illustrated)

imposing electric machine with a nominal power of $1.5\ kW$ and can provide a difference in torque at the wheels of about $600\ Nm$. Test drives with the MUTE vehicle showed that a difference in torque of $300\ Nm$ is sufficient to cover most of the occurring operating conditions, so that the torque load of the superimposing gear unit and the superimposing electric machine were reduced for the transmission CS03. The easiest way, without changing the concept or the assembly in doing so, is to reduce the tooth width of the superimposing gears. As the tooth width of the CS02 superimposing gears are already $5\ mm$, a further reduction of the tooth width is not reasonable for manufacturing reasons. This is why PPS GF 40 plastic gears instead of steel gears are integrated with a tooth width of $8\ mm$, designed according to VDI 2736 [12]. The VDI 2736 provides a proof of the load carrying capacity for thermoplastic polymers covering fatigues such as tooth breakage and pitting as well as the calculation of permissible deformations. To avoid a tooth breakage of the superimposing planet gears for the CS03, the torque load of each meshing is reduced by increasing the number of planet gears from 3 to 5 (see Fig. 9). Although the lightweight torque-vectoring unit (CS03) consists of more planet gears with a greater tooth width, the CS03 superimposing unit is lighter than that of CS02, thanks to the lower density of plastic and further component optimizations. Due to good sliding characteristics for the combination steel and plastic, no rolling contact bearings are applied between the planet gears and the planet bolts. Furthermore, the application of plastic gears has a positive influence on the noise emission of the torque-vectoring unit, as plastic features better damping characteristics than steel.

C. Reinforced plastic housing

The layout of the housing for the transmission CS03 is derived from the aluminium housing of the first VISIO.M transmission CS02. It features the same interface to the periphery but an optimized structure in terms of the load carrying capacity and deformations to meet the tightened manufacturing requirements for an injection molding. The nominal weight reduction gained by the substitution from an aluminium housing to a plastic housing for the VISIO.M transmission is approximately $40\ \%$. Numerical simulations of the applied reinforced plastic Vestamid HTplus were conducted for the fully loaded housing to evaluate the load carrying capacity and the elastic deformations. Whereas the load carrying capacity was proofed for all operating conditions, the deformations at certain areas reached values beyond the permissible limits, so that the housing had to be reinforced in these areas. Thus, a housing weight reduction of about $25 - 30\ \%$ is realistic.

D. Parking lock

The VISIO.M power train features a novel parking lock, designed and developed by the project partner Amtek Tekfor Holding. The parking lock is positioned at the drive pinion of the axle drive (see Fig. 10) and features a very compact design in comparison to conventional parking locks. A further advantage of this parking lock are the low rotating masses in comparison to solutions with a ratch wheel mounted on the shaft. The functionality of the parking lock is presented in the following. A lock ring, which sits coaxially to the pinion axis and is axially guided in the housing, features a spline contour at the outer surface to lock the rotation of the locking ring. By actuating the drive of the parking lock, the bearing at the end of the drive spindle rolls up on the ramp of the locking ring and presses the locking ring into the direction of the pinion shaft. Both the locking ring and the pinion shaft feature a conical contour, which provides a form closure between both

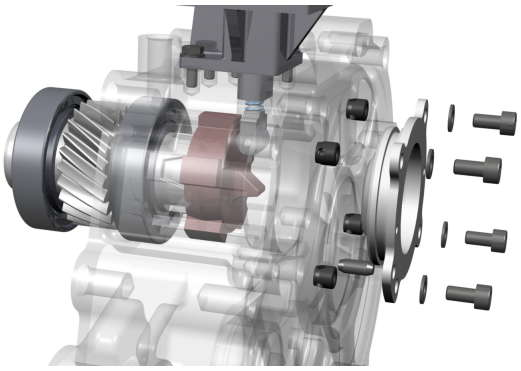

Fig. 10. Parking lock of transmission CS02

components when the locking ring is engaged. The axle drive is then locked. If there is tooth on tooth contact during the engaging process between the locking ring and the pinion shaft, so that the locking ring cannot be engaged, a spiral spring at the drive spindle pretensions the locking ring. So, if the vehicle is moving, the locking ring is engaging into the pinion shaft and ensures a save locking of the axle drive. The parking lock can be engaged for road gradients up to 30 % and vehicle speeds up to 5 km/h and is refused by the pinion shaft in the other case.

E. Comparison of Weight and Costs

Fig. 11, 12 and 13 show the weights of the transmission construction stages CS01, CS02 and CS03 broken down according to the assembly groups. The VISIO.M transmission reaches a weight reduction of 7 % in comparison to the CS01 transmission although the torque load of both the axle drive and the torque-vectoring unit have been increased. Only the torque-vectoring unit (TV-unit) got minimally heavier due to the increase of the torque-vectoring gear ratio and a superimposing torque motor with a higher elasticity in terms of the availability of the maximum difference in torque at the driven wheels. Nevertheless, the application of a modular superimposing electric machine reduces the costs disproportionately in contrast to the hollow shaft electric motor of the CS01. The weight reduction of the other assembly groups mainly results from the component optimizations. The application of a reinforced plastic housing for the CS03 transmission reduces the weight for a further 1.5 kg. The restriction of the torque-vectoring power in combination with the integration of plastic gears saves 1 kg for the torque-vectoring unit. Both housings of the CS02 (aluminium) and CS03 (reinforced plastic) can be manufactured through an injection molding process and can save costs for larger lot sizes. A further advantage of the CS03 torque-vectoring unit is the low production costs of the PPS GF 40 planet gears. Only one type of planet gear with the same involute shape, each manufactured in one process step, is used for all planetary gear trains of the superimposing unit.

IV. Optimization of the Axle Drive Excitation Level

A. Noise emission of gear trains and tooth force level

Each running gearing excites an oscillation, which results in an excitation frequency dependent on the number of teeth of the gear z and the speed n:

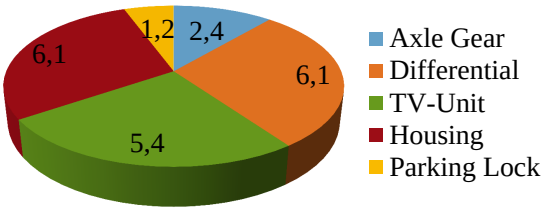

Fig. 11. Weight distribution MUTE transmission CS01

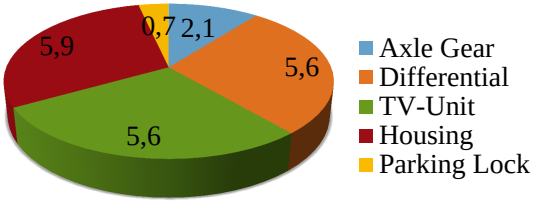

Fig. 12. Weight distribution VISIO.M transmission CS02

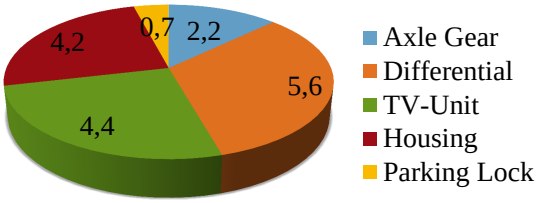

Fig. 13. Weight distributionVISIO.M transmission CS03

$$f_z = \frac{n \cdot z}{60} \tag{3}$$

In particular, the dynamic tooth force has a significant influence on the oscillation, which is alternating over the time, depending on how many gears are in contact at the present time. Further influence on the excitation of a gearing are manufacturing deviations at the tooth flank. On the other hand, targeted modifications on the tooth flank can reduce the excitation level of a gearing. A critical operating condition appears if an excitation frequency occurs near resonant frequencies and results in undesirably high oscillation amplitudes. The magnitude of the oscillation amplitude then is specified by the distance between the excitation and resonant frequency, the intensity of the excitation and the effective damping. The tooth force level L_{Fz} is a model-based parameter, which is used to evaluate the excitation level of a gearing during the design process. The tooth force level only considers the gearing itself and not the oscillation characteristic of the gearbox. Nevertheless, a correlation between the excitation and the oscillation response can be met. It is valid that a reduction of the excitation directly involves a qualitative and quantitative related reduction of the oscillation response (i. e. noise emission).

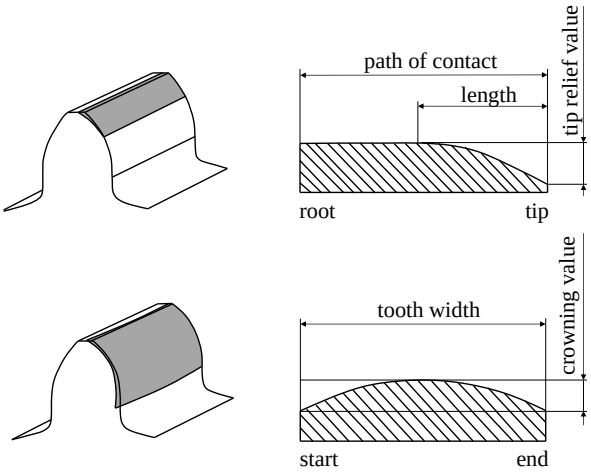

Fig. 14. Tooth flank profile modification

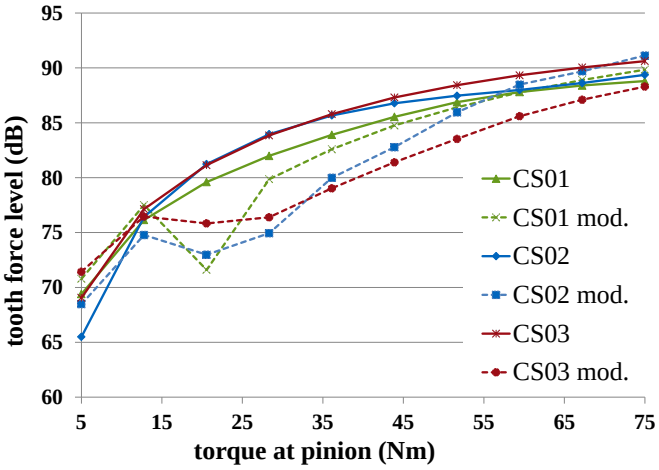

Fig. 15. Tooth force level CS01-CS02-CS03 of axle drive stage 1 with unmodified and modified (mod.) profile

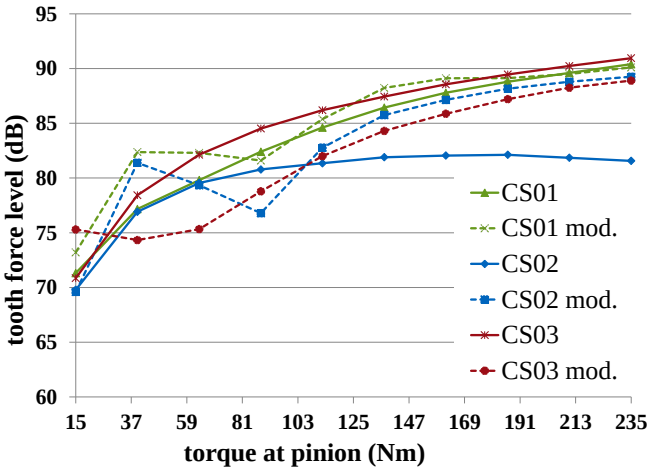

Fig. 16. Tooth force level CS01-CS02-CS03 of axle drive stage 2 with unmodified and modified (mod.) profile

B. *Determination of the profile modification*

The goal of a tooth profile modification of gears is to reduce the noise excitation [13], i. e. the tooth force level, and to ensure a smooth load distribution at the tooth flank on the other hand. An irregular load distribution of the unmodified tooth flank can be caused by effects such as process tolerances, different bearing clearances and shaft deformations. To achieve a smooth load distribution, the designer generally tries to unload the tooth root and tip of high Hertzian stress levels. Unfortunately, both design requirements cannot both be satisfied optimally, so that a compromise between a reduction of the excitation and a smooth load distribution has to be designed iteratively.

Conventional profile modifications are the tip relief and the crowning (see Fig. 14), which were designed and applied to the gearings of the VISIO.M transmission. The tip relief is definied by the amount of correction (amount of the nominal involute shape in μm to be ground down) and the modification length along the profile, whereas the circular crowning is only definied by the amount of correction.

C. *Comparison of tooth force level*

In the following, the tooth force level of the axle drive stages 1 & 2 for each transmission construction stage will be compared. The tooth force level is calculated for discrete torque values within the operating range of the drive motor. For each stage and construction stage two calculations were conducted. On the one hand the gearing without any profile modification on the tooth flank and on the other hand with a predefined profile modification (tip relief and crowning). The unmodified tooth force level of a gearing generally shows a logarithmic increase over the torque. By applying a profile modification to the tooth flank it is possible to reduce the tooth force level at a specific design point or area respectively. Besides the profile modification in terms of a low tooth force level, the designer has to determine a profile modification resulting in a smooth load distribution on the tooth flank. Thus, the design of a profile modification usually represents a compromise between a low tooth force level and a smooth load distribution. The design point torque in terms of the tooth force level corresponds to a driving condition of the vehicle with the highest time slice of the load spectrum. For the VISIO.M vehicle the driving condition at $50\ km/h$ was chosen to be acoustically optimized, so that an unremarkable noise emission of the gearbox can be expected at this operating point.

For the first stage of the axle drive all construction stages show a similar logarithmic increase and value of the tooth force level over the pinion torque for the unmodified tooth flanks (see Fig. 15). As the occurring load distribution on the tooth flank is uncritical for the first gear stage, the determination of the profile modifications was only designed with respect to a reduction of the tooth force level.

CS01 shows the lowest tooth force level at the design point of the modified profiles, whereas the other variants feature a distinct minimum in a wider area around the design point.

Axle drive stage 2 features higher Hertzian stresses, so that the profile modifications could not only be determined in terms of a low tooth force level but to provide a smooth load distribution on the tooth flank as well. It has to be noticed that the unmodified profile of CS02 already shows a very low tooth force level for all acting torques. This relates to the already beneficial geometrical parameter of the gearing for the unmodified profile, significantly influenced by the applied helix angle or rather the overlap ratio ϵ_β. The helix angle of the second stage of transmissions CS01 and CS02 was determined in the way that the resulting axial force on the intermediate shaft compensates the axial force resulting from the gearing of stage 1. Nevertheless, the tooth profiles of the second stage had to be modified in terms of a smooth load distribution, which leads to worse tooth force levels of the modified profiles of CS01 and CS02 in comparison to the unmodified profile. Due to an axial force free gearing in CS03, the helix angle could be chosen in such a way that a smooth load distribution and a low tooth force level results for the modified profile.

V. Conclusion

During the MUTE and VISIO.M research project three transmissions were designed and manufactured. Each of them features nearly the same gear layout, such as a 2-stage axle drive, a spur gear differential and a torque-vectoring unit to variably control and distribute the torque at each driven vehicle wheel. The main development goal of the first VISIO.M transmission CS02 was put on the reduction of weight and costs using conventional materials and gear concepts. The optimization of components led to a weight reduction of approximately 7 % in comparison to transmission CS01. Due to high requirements on the driving dynamics for the demonstrator vehicle, the power input of the superimposing machine had to be raised remarkably. Although the implemented superimposing machine reaches high differences in torque at the driven wheels, i. e. for demonstration purposes, a reduced input power is sufficient to raise the recuperation level of the drive motor, which was the primarily development target of the torque-vectoring system. This is why a second ultra-lightweight transmission CS03 was designed during the VISIO.M project, doing research on new materials to further reduce the weight. Therefore, a reinforced plastic housing was applied instead of an aluminium housing for the lightweight transmission CS03. As the yield stress of plastic is clearly lower than that of aluminium, it is necessary to reduce the load on the housing caused by the tooth forces of the gears. Especially axial forces of helical gears, which are used in conventional axle drives to reduce the noise excitation of the transmission, lead to high bending torques and thus high deformations in a plastic housing. To avoid this additional load on the housing, a new gear concept was applied to the axle drive of the lightweight transmission. Both stages of the axle drive feature a herringbone gearing, where two helical gears with opposite helix angle are applied to each shaft of a gearing. The acting axial forces of the two gears cancel each other and do not load the housing. Thus, this gear concept with double-helical gears makes the application of lightweight materials possible and comes along with a low noise excitation none the less.

References

[1] B.-R. Hoehn, K. Stahl, P. Gwinner, and F. Wiesbeck, "Torque-Vectoring Driveline for Electric Vehicles," in *Proceedings of the FISITA 2012 World Automotive Congress*, ser. Lecture Notes in Electrical Engineering. Springer Berlin Heidelberg, 2012, vol. 191, pp. 585–593.

[2] B.-R. Hoehn, K. Stahl, M. Lienkamp, C. Wirth, F. Kurth, and F. Wiesbeck, "Electromechanical Power Train with Torque Vectoring for the Electric Vehicle MUTE of the TU München," in *VDI-Berichte 2130*, ser. Transmissions in Vehicles. Springer Berlin Heidelberg, 2011, pp. 77–94.

[3] L. De Novellis, A. Sorniotti, P. Gruber, L. Shead, V. Ivanov, and K. Hoepping, "Torque Vectoring for Electric Vehicles with Individually Controlled Motors: State-of-the-Art and Future Developments." Los Angeles, CA, USA: 26th International Electric Vehicle Symposium (EVS26), 2012.

[4] L. De Novellis, A. Sorniotti, and P. Gruber, "Design and Comparison of the Handling Performance of Different Electric Vehicle Layouts." Journal of Automobile Engineering, 2013.

[5] T. C. Meißner, "Verbesserung der Fahrzeugquerdynamik durch variable Antriebsmomentenverteilung," Ph.D. dissertation, Audi Dissertationsreihe, Cuvillier Verlag Göttingen, 2008.

[6] M. Graf, F. Wiesbeck, and M. Lienkamp, "Fahrwerks- und Torque-Vectoring-Entwicklung für das Fahrzeug MUTE," *ATZ Heft 6*, vol. 113, 2011.

[7] K. Sawase and Y. Ushiroda, "Improvement of Vehicle Dynamics by Right-and-Left Torque Vectoring System in Various Drivetrains." Society of Automotive Engineers of Japan, 2008.

[8] T. Smetana, T. Bierman, B.-R. Höhn, F. Kurth, and C. Wirth, "The Active Differential for Future Drive Trains." Schaeffler Symposium, 2010.

[9] R. Denzler, C. Granzow, R. Peter, and M. Spieß, "Das Hinterachsgetriebe Vector Drive," *ATZ*, vol. 109, pp. 1106–1115, 2007.

[10] B.-R. Hoehn, C. Wirth, and F. Kurth, "Electric Axle Drive with Torque-Vectoring-Functionality," *VDI-Berichte*, vol. 2081, pp. 581–597, 2010.

[11] B.-R. Hoehn, K. Stahl, C. Wirth, M. Lienkamp, F. Kurth, and F. Wiesbeck, "Elektromechanisches Torque-Vectoring mit aktivem Differential zur Maximierung der Rekuperationsfähigkeit," in *2. Automobiltechnisches Kolloquium Garching 11./12. April 2011*, 2011.

[12] VDI 2736, "Thermoplastische Zahnräder (draft)." Beuth-Verlag, Berlin, 2013.

[13] B.-R. Hoehn, P. Oster, S. Radev, and T. Griggel, "Zahnflankenkorrekturen gegen Geräuschanregung von Stirnrädern in Theorie und Praxis. Auslegung geräuscharmer Vrzahnungen mit dem EDV-Programm DZP ("Dynamische Zahnkräfte Programm")," in *VDI-Berichte 1968*. Verein Deutscher Ingenieure (VDI), 2006, pp. 235–250.